Synergistic Effects of Olive Oil Ash as Supplementary Cementitious Material and Recycled Concrete Aggregates on Concrete Performance under Water Curing and Internal Curing Regimes

Siwar Khasawneh[1] . Ayat Khasawneh[1]

[1] School of Civil Engineering, Universiti Sains Malaysia, Penang, Malaysia

siwar.khasawneh@gmail.com , ayatrasme@yahoo.com

Corresponding author: siwar.khasawneh@gmail.com

ACCEPTED MANUSCRIPT

Abstract

This study investigates the combined effects of olive oil ash (OOA) as a partial cement replacement (0–15% by binder weight) and recycled concrete aggregate (RCA) at 0%, 50%, and 100% replacement of natural coarse aggregate on the fresh, mechanical, durability, shrinkage, and microstructural properties of concrete. A total of 24 mixtures were prepared, including 12 subjected to conventional water curing (WC) and 12 to internal curing (IC) using pre-saturated RCA, all with a constant water-to-binder ratio of 0.45. Fresh properties evaluated included slump, air content, density, and setting time, while hardened properties comprised compressive strength, tensile and flexural strength, modulus of elasticity, permeability, porosity, RCPT, water absorption, shrinkage, UPV, and density. XRD analysis was conducted to identify hydration products. Results showed that 5% OOA maintained or enhanced strength, whereas 15% reduced it by 5–8%. Internal curing increased 56-day strength by up to 9.1% and improved durability, reducing permeability, porosity, and RCPT by up to 8.9%. XRD confirmed enhanced C–S–H formation at 5% OOA. Statistical analysis ($p < 0.001$, $R^2 = 0.94$) validated the significance of all variables. The optimized mix reduced CO_2 emissions by ~18% (preliminary estimate) while maintaining performance.

Keywords: Recycled concrete aggregate; Olive oil ash; Internal curing; XRD analysis; Shrinkage

1. Introduction

The construction industry consumes enormous quantities of natural resources each year, with global concrete production exceeding 14 billion cubic metres annually. This demand places significant pressure on natural aggregate extraction and cement manufacturing, both of which are major contributors to anthropogenic carbon dioxide emissions. The use of recycled concrete aggregate (RCA) derived from construction and demolition waste has therefore emerged as an effective strategy to reduce aggregate depletion, while the partial replacement of ordinary Portland cement (OPC) with supplementary cementitious materials (SCMs) helps lower the carbon footprint associated with binder production [1,2].

RCA differs from natural coarse aggregate (NCA) mainly due to the presence of adhered mortar surrounding the original aggregate particles. This residual mortar increases porosity and water absorption and introduces additional interfacial transition zones (ITZs), which generally lead to reductions in mechanical strength and durability when RCA fully replaces NCA without appropriate mitigation measures [3,22]. The extent of performance deterioration is typically proportional to the level of RCA replacement and depends strongly on the quality of the parent concrete and the processing techniques used during recycling [26].

Internal curing (IC) has been widely recognized as an effective method for supplying additional moisture to the cementitious matrix from within, thereby sustaining hydration reactions that may otherwise cease under sealed or inadequate external curing conditions. The pre-saturation of porous lightweight aggregates, or alternatively the utilization of the inherent porosity of RCA as an internal water reservoir, has been reported to reduce autogenous shrinkage, enhance microstructural densification, and improve long-term strength development [4–6]. This approach is particularly beneficial for RCA concrete, where the high absorption capacity of recycled aggregates can be transformed from a limitation into a functional advantage.

Olive oil ash (OOA), a biomass combustion by-product generated during olive pomace energy recovery, has recently attracted attention as a potential supplementary cementitious material. However, its chemical composition does not satisfy the requirements for classification as a pozzolan under ASTM C618. Therefore, OOA is considered in this study to contribute primarily through a filler effect, with possible limited pozzolanic and/or latent-hydraulic reactivity associated with its amorphous silica and relatively high CaO content. Its high specific surface area may further contribute to particle packing and pore refinement within the cementitious matrix [9,10].

Although RCA utilization, internal curing, and SCM incorporation have each been studied individually, investigations addressing the combined interaction of these three parameters remain limited. In particular, quantitative evaluations of biomass-derived pozzolans such as OOA in RCA concrete under different curing

ACCEPTED MANUSCRIPT

regimes are scarce, and their influence on hydration products identifiable through X-ray diffraction (XRD) analysis has not been sufficiently explored.

Accordingly, the objectives of this study are threefold: (i) to quantify the influence of four OOA replacement levels (0%, 5%, 10%, and 15%) on the mechanical, durability, and shrinkage properties of concrete incorporating three RCA replacement levels (0%, 50%, and 100%); (ii) to evaluate the effectiveness of internal curing using pre-saturated RCA compared with conventional water curing; and (iii) to correlate macroscopic performance with mineralogical changes identified through XRD analysis. The experimental programme comprises 24 concrete mixtures and more than 20 measured properties, providing a comprehensive dataset for the development of sustainable recycled aggregate concrete. Unlike previous studies that investigated these parameters in isolation, the present work systematically evaluates the combined influence of OOA, RCA at multiple replacement levels, and internal curing. The novelty extends to: (a) correlation analysis between microstructural indicators and macroscopic performance, (b) XRD-based qualitative interpretation of the OOA–IC interaction, and (c) a preliminary sustainability assessment of the CO_2-reduction potential of the optimized mixture.

2. Materials and Methods

2.1. Constituent Materials

Ordinary Portland cement (OPC) conforming to ASTM C150 Type I was used as the primary binder [12]. Its chemical composition, determined by X-ray fluorescence (XRF), is presented in Table 2. The cement had a specific gravity of 3.15, a median particle size (d_{50}) of 6.77 μm, and a Blaine specific surface area (SSA) of 0.378 m^2/g.

Olive oil ash (OOA) was sourced from an olive pomace combustion facility, collected after electrostatic precipitation, and ground in a ball mill until the D_{50} reached 50 μm. The OOA had a specific gravity of 1.80, an SSA of 25.0 m^2/g (measured by nitrogen adsorption using the BET method), and a combined SiO_2 + Al_2O_3 + Fe_2O_3 content of 28.2% (Table 2). This value is below the minimum chemical requirements specified by ASTM C618 for Class N (70%) and Classes F and C (50%). Accordingly, OOA does not satisfy the chemical composition requirements for classification under ASTM C618. Given its relatively high CaO content (30.3%), OOA is considered in this study to contribute primarily through a filler effect, with possible limited pozzolanic and/or latent-hydraulic reactivity.

Natural coarse aggregate (NCA) was crushed limestone with a maximum nominal size of 20 mm, a specific gravity (SSD) of 2.52, and a water absorption of 1.05%. Recycled concrete aggregate (RCA) was obtained by crushing laboratory-cast concrete specimens (cubes, beams, and arch elements previously cast and tested at Universiti Sains Malaysia, USM; original design strength = 35 MPa, age > 365 days) to a grading similar

ACCEPTED MANUSCRIPT

to that of the NCA. Because this RCA was derived from controlled laboratory specimens rather than field construction and demolition waste (CDW), its attached-mortar content, gradation uniformity, and impurity profile are expected to be more consistent than those of typical CDW-derived RCA. Therefore, the findings of this study should be interpreted within this limitation, and further investigation using field-sourced CDW-RCA is recommended to confirm their broader applicability. The RCA had a specific gravity (SSD) of 2.40, a water absorption of 4.70%, an LA abrasion loss of 25.0%, and an aggregate crushing value of 30.26% (Table 1). Natural river sand with a fineness modulus of 2.65 and specific gravity of 2.52 served as the fine aggregate.

A polycarboxylate-ether (PCE) based superplasticizer in brown liquid form (solid content ≈ 30%) was used to maintain workability across all mixtures, with dosage adjusted to compensate for the increased water demand caused by OOA fineness and RCA surface roughness.

Table 1. Physical and mechanical properties of the coarse aggregates (NCA and RCA). Properties are reported in the text of Section 2.1.

Property	NCA	RCA	Unit
Specific gravity (SSD)	2.52	2.40	-
Water absorption	1.05	4.70	%
LA abrasion loss	13.0	25.0	%
Unit weight	1620	1270	kg/m^3
Aggregate crushing value	22.12	30.26	%

Table 2. Chemical composition and physical properties of OPC and OOA

Property	OPC	Olive Oil Ash (OOA)	Unit
SiO_2	21.10	21.20	%
Al_2O_3	3.30	4.40	%
Fe_2O_3	2.91	2.60	%
CaO	68.04	30.30	%
$SiO_2 + Al_2O_3 + Fe_2O_3$	27.31	28.20	%

ACCEPTED MANUSCRIPT

Specific gravity	3.15	1.80	-
d_{50}	6.77	50.0	μm
SSA	0.378	25.0	m^2/g

Figure 1 shows the laboratory-cast concrete specimens (cubes, beams, and arch elements previously cast and tested at USM) used as the source material for RCA production prior to crushing. The visible adhered mortar and angular fracture surfaces are characteristic of crushed hardened concrete, and the exposed reinforcement steel originates from the reinforced beam and arch specimens rather than from demolished in-service structures.



Figure 1: Laboratory-cast concrete specimens (cubes, beams, and arch elements, previously tested at USM) before crushing for RCA production.

The particle size distribution of RCA after crushing and sieving is illustrated in Figure 2. The fractions displayed correspond to sieve sizes of 5 mm, 2.36 mm, 1.18 mm, 0.6 mm, 0.3 mm, 0.15 mm, 0.076 mm, and pan, confirming compliance with ASTM C33 grading requirements [11].

ACCEPTED MANUSCRIPT



Figure 2: Sieve analysis fractions of recycled concrete aggregate showing particle size distribution.

2.2. Mix Design

Twenty-four concrete mixtures were designed following a full factorial arrangement of three factors: RCA replacement level (0%, 50%, 100% of natural coarse aggregate by mass), OOA replacement level (0%, 5%, 10%, 15% of total binder by mass), and curing regime (water curing, WC; internal curing, IC). The total binder content was held constant at 380 kg/m^3 and the effective water-to-binder ratio at 0.45 for all mixtures. RCA was used in the saturated surface-dry (SSD) condition to prevent absorption of mix water; for internally cured specimens, the RCA was additionally pre-soaked for 24 hours and surface-dried before batching to serve as an internal moisture reservoir. The pre-absorbed water was approximately 22.3 kg/m³ for the R50 mixtures and 44.7 kg/m³ for the R100 mixtures, based on the RCA water absorption of 4.70%. This water was additional to the 171 kg/m³ of design mixing water and was not included in the nominal effective w/b ratio of 0.45 because it was initially stored within the RCA pores. For transparency, Table 3 separately reports the design mixing water, pre-absorbed internal-curing water, and total water content.

Table 3. Concrete mix proportions (per m³)

Component	R0-O0	R0-O5	R0-O10	R0-O15	R50-O0	R50-O5	R50-O10	R50-O15	R100-O0	R100-O5	R100-O10	R100-O15	Unit
OPC	380	361	342	323	380	361	342	323	380	361	342	323	kg/m³

ACCEPTED MANUSCRIPT

OOA	0	19	38	57	0	19	38	57	0	19	38	57	kg/m³
NCA (dry)	950	950	950	950	475	475	475	475	0	0	0	0	kg/m³
RCA (SSD)	0	0	0	0	475	475	475	475	950	950	950	950	kg/m³
Sand (dry)	680	680	680	680	680	680	680	680	680	680	680	680	kg/m³
Water (eff.)	171	171	171	171	171	171	171	171	171	171	171	171	kg/m³
w/b	0.45	0.45	0.45	0.45	0.45	0.45	0.45	0.45	0.45	0.45	0.45	0.45	-
PCE SP (%)	0.40	0.55	0.70	0.85	0.55	0.70	0.85	1.00	0.70	0.85	1.00	1.15	%
Total water*	171	171	171	171	193.3	193.3	193.3	193.3	215.7	215.7	215.7	215.7	kg/m³

*Pre-absorbed IC water and total water values apply to internally cured (IC) mixtures. For water-cured (WC) mixtures, the pre-absorbed IC water is zero and the total water content is 171 kg/m³.

2.3. Specimen Preparation and Curing Regimes

Concrete was mixed in a 120-litre pan mixer following a standard sequence: dry mixing of aggregates and binder for 60 seconds, addition of 70% of mix water and mixing for 90 seconds, addition of remaining water with superplasticizer and mixing for a further 120 seconds. Fresh property tests were conducted immediately after mixing. Specimens were cast in steel moulds, compacted on a vibrating table for 15 seconds per layer (two layers), and demoulded after 24 hours. WC specimens were immersed in a lime-saturated water tank at 23 ± 2 °C until the age of testing. IC specimens were wrapped in wet hessian and polyethylene sheeting for the first 7 days, then stored in a controlled environment at 23 ± 2 ℃° and 50 ± 5% relative humidity, relying on the moisture released from pre-saturated RCA pores for continued internal hydration.

ACCEPTED MANUSCRIPT

2.4. Test Methods

For each hardened property and at each test age, three replicate specimens were prepared and tested, and the reported value represents the arithmetic mean of the three measurements. Fresh concrete properties were assessed following ASTM standards: slump (ASTM C143), air content by pressure method (ASTM C231), fresh density (ASTM C138), and setting time by penetration resistance (ASTM C403). Compressive strength was measured on 100 × 200 mm cylinders at 7, 28, and 56 days (ASTM C39) [13]. Splitting tensile strength (ASTM C496) [14], flexural strength on 100 × 100 × 400 mm prisms (ASTM C78) [15], and static modulus of elasticity (ASTM C469) [16] were determined at 28 days.

Durability testing at 28 days included: water permeability by penetration depth under 5 bar pressure (DIN 1048), total porosity by vacuum saturation (ASTM C642), rapid chloride penetration test (ASTM C1202) [17], water absorption by immersion (ASTM C642), and initial sorptivity (ASTM C1585) [18]. Drying shrinkage was measured on 75 × 75 × 285 mm prisms (ASTM C157) at 28 and 56 days [19]; autogenous shrinkage was monitored from the time of final set to 7 days using sealed corrugated tubes. Ultrasonic pulse velocity (UPV) was measured at 28 days (ASTM C597) [20], and hardened density was determined by dimensional measurement and mass.

X-ray diffraction (XRD) analysis was performed on powder samples extracted from the cores of 28-day specimens using a Cu-Kα radiation source ($\lambda = 1.5418$ Å) at 40 kV and 40 mA. Scans covered a 2θ range of 5–65° with a step size of 0.02° and a dwell time of 1 second per step.

ACCEPTED MANUSCRIPT

3. Results and Discussion

3.1. Fresh Concrete Properties

The fresh concrete properties were identical for both curing regimes since the curing protocol commenced after casting. Slump values ranged from 100 mm (R100-O0) to 140 mm (R0-O15), indicating that increasing OOA content improved workability despite the higher PCE dosage required. This can be attributed to the spherical morphology and lubricating effect of fine OOA particles, which reduce inter-particle friction. Conversely, increasing RCA content from 0% to 100% decreased slump by 15–18 mm at each OOA level, consistent with the rough, angular surface texture of RCA and the absorption of free water by adhered mortar even in the SSD condition [3].

Fresh density decreased systematically from 2310 kg/m³ (R0-O0) to 2180 kg/m³ (R100-O15), reflecting the lower specific gravity of both RCA (2.40 vs 2.52 for NCA) and OOA (1.80 vs 3.15 for OPC). Air content increased marginally from 1.9% to 2.5% across the full matrix, with both RCA and OOA contributing to entrapped air through increased particle angularity and carbon residue in the ash. Setting times were prolonged by both OOA and RCA: initial setting time extended from 185 min (R0-O0) to 238 min (R100-O15), attributable to the dilution of clinker phases by OOA and the retarding effect of dissolved ions from RCA adhered mortar [7].

The PCE superplasticizer dosage required to maintain the target workability increased markedly with RCA and OOA content, from 0.40% by binder mass in R0-O0 (1.52 kg/m³) to 1.15% in R100-O15 (4.37 kg/m³) an almost threefold increase driven by the higher water demand of the fine OOA particles and the rough, absorptive surface of the RCA. This dosage was established by trial batches targeting a constant slump range rather than by a fixed addition. Two practical implications follow. First, dosages approaching the upper end carry a risk of segregation, bleeding, or set retardation; in the present mixtures the measured air content increased only modestly (from 1.9% to 2.5%) and no segregation was observed, but air content was not actively controlled with an air-entraining admixture, and the highest dosage (1.15%) should be verified against the manufacturer's recommended maximum for the specific product to avoid overdosing. Second, PCE is among the more costly concrete constituents, so a threefold dosage increase carries a non-trivial cost and embodied-carbon penalty that partially offsets the sustainability benefit of the mixture; this trade-off should be weighed in any practical specification and is minimised by keeping OOA at the 5% optimum, where the required dosage is substantially lower than at 15%.

ACCEPTED MANUSCRIPT

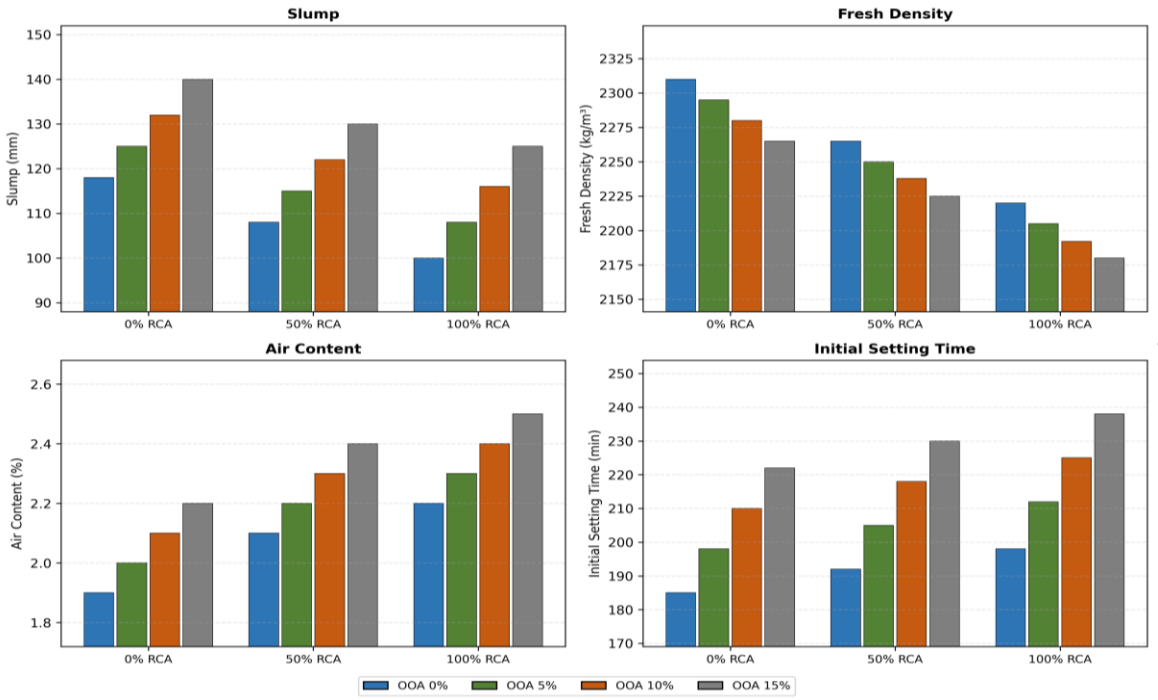


Figure 3: Fresh concrete properties as a function of RCA and OOA content.

3.2. Compressive Strength

The compressive strength results at 7, 28, and 56 days under both curing regimes are summarized in Table 4 and illustrated in Figures 4&5. At 28 days under water curing, the control mix R0-O0 achieved 32.0 MPa, while full RCA replacement (R100-O0) reduced strength to 26.0 MPa, representing an 18.8% reduction. This decline is attributed to the weaker ITZ between the old adhered mortar and the new cement paste, as well as the increased porosity of RCA particles [22, 24]. In RCA concrete, two distinct ITZs exist: the original ITZ between the parent aggregate and adhered mortar, and the new ITZ between the adhered mortar and fresh cement paste. The new ITZ is typically more porous due to the wall effect caused by the rough, porous surface of the adhered mortar, which leads to localized accumulation of bleed water and reduced packing density of cement grains [24, 34]. This dual-ITZ system represents the primary microstructural weakness in RCA concrete and is the target of both pozzolanic refinement by OOA and densification through internal curing.

The incorporation of 5% OOA consistently enhanced or maintained 28-day compressive strength across all RCA levels: R0-O5 reached 32.5 MPa (+1.6% over R0-O0), R50-O5 reached 29.0 MPa (+1.8% over R50-O0), and R100-O5 reached 26.5 MPa (+1.9% over R100-O0) under WC. This improvement is attributed to the filler effect and moderate pozzolanic reaction of OOA at low replacement levels, which refines the pore structure without significantly diluting the clinker content [8, 10]. Because these differences are small (of the order of 1–2%), they should be interpreted with caution pending formal statistical testing of the

ACCEPTED MAN

replicate-specimen data; the practical significance of the 5% OOA dosage lies primarily in maintaining strength while replacing part of the cement, rather than in a large absolute gain. At 10% OOA replacement, strength remained comparable to or slightly below the 0% OOA reference, while 15% OOA resulted in reductions of 7.8%, 7.0%, and 7.7% for R0, R50, and R100 groups respectively, indicating that the dilution effect outweighed pozzolanic gains at this dosage.

Internal curing produced measurable strength improvements at all ages, with the gains amplifying over time. At 7 days, IC specimens showed only 0.5–1.3 MPa improvements, reflecting the early onset of internal moisture release. By 56 days, the IC advantage was most pronounced in 100% RCA mixes: R100-O0 increased from 28.5 MPa (WC) to 31.1 MPa (IC), a 9.1% gain; R100-O5 rose from 29.5 MPa to 32.2 MPa (+9.2%). The mechanism underpinning this improvement is the sustained release of absorbed water from RCA pores, which maintains a high internal relative humidity in the paste, promoting continued hydration of residual anhydrous cement and pozzolanic reaction of OOA with portlandite [4, 6].

Table 4*. Compressive strength (MPa) under water curing (WC) and internal curing (IC)

Mix (R% – O%)	7 Days		28 Days		56 Days	
	WC	IC	WC	IC	WC	IC
R0-O0	22.0 ± 0.9	22.2 ± 0.9	32.0 ± 1.0	32.3 ± 1.0	34.5 ± 1.2	34.8 ± 1.2
R0-O5	21.5 ± 0.3	21.7 ± 0.3	32.5 ± 1.3	32.8 ± 1.3	35.5 ± 1.2	35.9 ± 1.2
R0-O10	20.8 ± 0.5	21.0 ± 0.5	31.5 ± 0.4	31.8 ± 0.4	35.0 ± 0.3	35.4 ± 0.3
R0-O15	19.5 ± 0.7	19.7 ± 0.7	29.5 ± 1.0	29.8 ± 1.0	33.5 ± 0.8	33.8 ± 0.8
R50-O0	19.5 ± 0.8	20.2 ± 0.8	28.5 ± 1.0	29.5 ± 1.0	31.0 ± 1.2	32.2 ± 1.2
R50-O5	19.2 ± 1.0	19.9 ± 1.0	29.0 ± 0.7	30.0 ± 0.7	32.0 ± 1.2	33.3 ± 1.2
R50-O10	18.8 ± 0.4	19.5 ± 0.4	28.2 ± 0.5	29.2 ± 0.5	31.5 ± 0.3	32.8 ± 0.3
R50-O15	17.8 ± 0.7	18.4 ± 0.7	26.5 ± 1.0	27.4 ± 1.0	30.0 ± 1.2	31.2 ± 1.2
R100-O0	18.0 ± 0.7	19.3 ± 0.7	26.0 ± 1.0	27.9 ± 1.0	28.5 ± 1.2	31.1 ± 1.2
R100-O5	18.0 ± 0.6	19.3 ± 0.6	26.5 ± 0.7	28.5 ± 0.7	29.5 ± 1.2	32.2 ± 1.2
R100-O10	17.5 ± 0.3	18.8 ± 0.3	25.5 ± 0.4	27.4 ± 0.4	29.0 ± 0.3	31.6 ± 0.3
R100-O15	16.5 ± 0.7	17.7 ± 0.7	24.0 ± 1.0	25.8 ± 1.0	27.5 ± 1.0	30.0 ± 1.0

*Values are expressed as mean ± SD (n = 3)

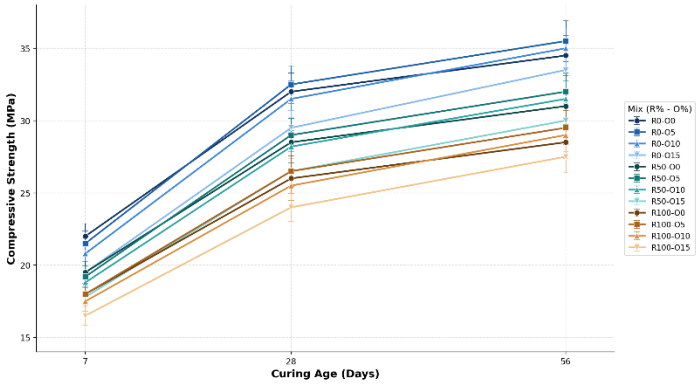


Figure 4: Compressive strength development at 7, 28, and 56 days (WC).

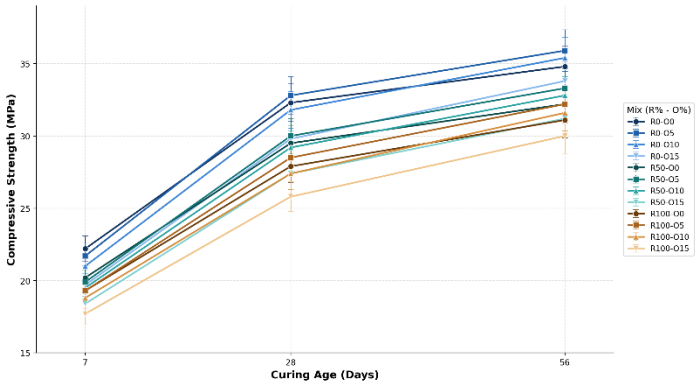


Figure 5 Compressive strength development at 7, 28, and 56 days (IC).

3.3. Splitting Tensile, Flexural Strength, and Modulus of Elasticity

At 28 days, splitting tensile strength under WC ranged from 2.05 MPa (R100-O15) to 2.75 MPa (R0-O5), while IC values ranged from 2.2 MPa (R100-O15) to 2.8 MPa (R0-O5). The ratio of splitting tensile to compressive strength remained within the expected range of 7.8–8.5% for normal-strength concrete, confirming consistent failure mechanisms across all mixtures [28]. The 5% OOA replacement improved tensile strength by 1.8–2.3% under both curing regimes, while 15% OOA reduced it by 6.8–7.4%.

Flexural strength followed analogous trends, ranging from 3.25 MPa (R100-O15 WC) to 4.30 MPa (R0-O5 under both regimes). The flexural-to-compressive strength ratio of approximately 12.5–13.5% remained consistent, indicating that neither RCA nor OOA fundamentally altered the tensile failure mode. IC improved flexural strength by 2.7–7.7% across the R100 group, with the greatest gain at R100-O5 (3.58 MPa WC vs. 3.80 MPa IC, +6.1%).

The static modulus of elasticity at 28 days decreased with increasing RCA content, from 28.5 GPa (R0-O0 WC) to 21.5 GPa (R100-O15 WC), a 24.6% reduction attributable to the lower intrinsic stiffness of the adhered mortar in RCA [22, 25]. OOA at 5% improved the modulus marginally (0.3–1.0 GPa) across all groups, while IC enhanced values by 0.1–0.9 GPa, with larger gains at higher RCA levels. The interaction between IC and OOA at 5% replacement produced the highest modulus within each RCA group.

ACCEPTED MANUSCRIPT

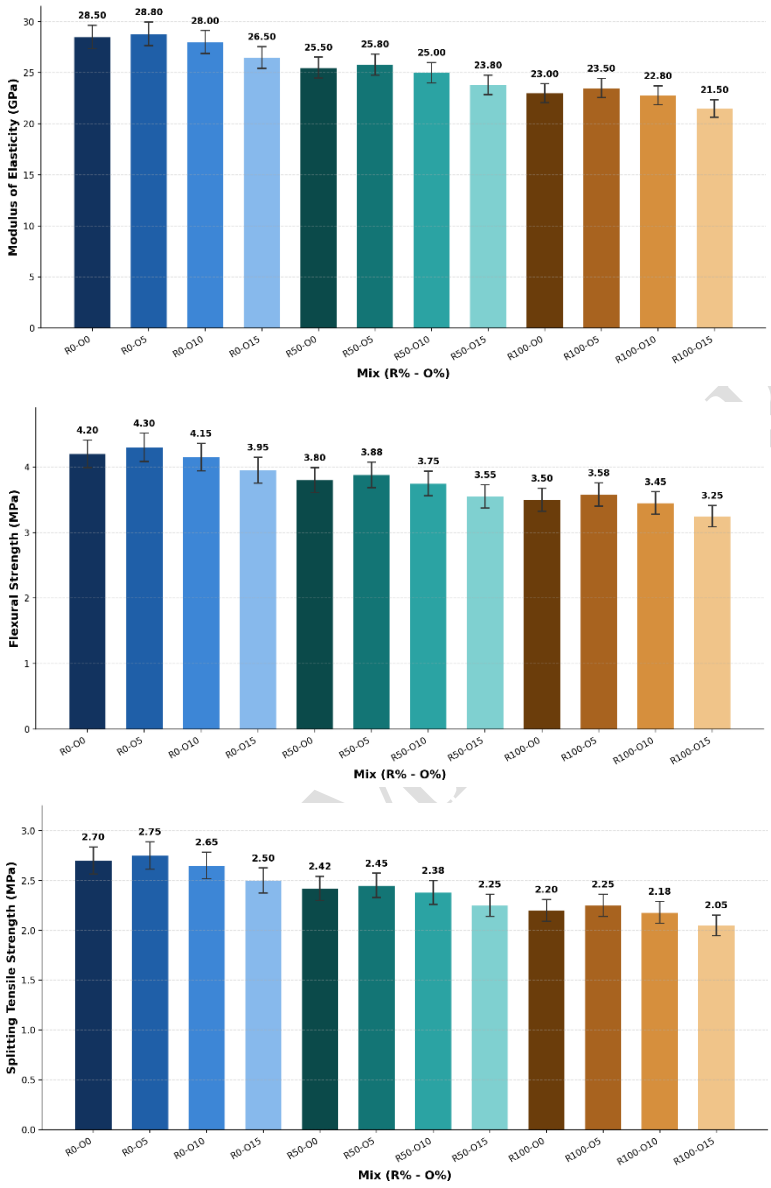


Figure 6: 28-day splitting tensile strength, flexural strength, and modulus of elasticity (WC).

ACCEPTED MANUSCRIPT

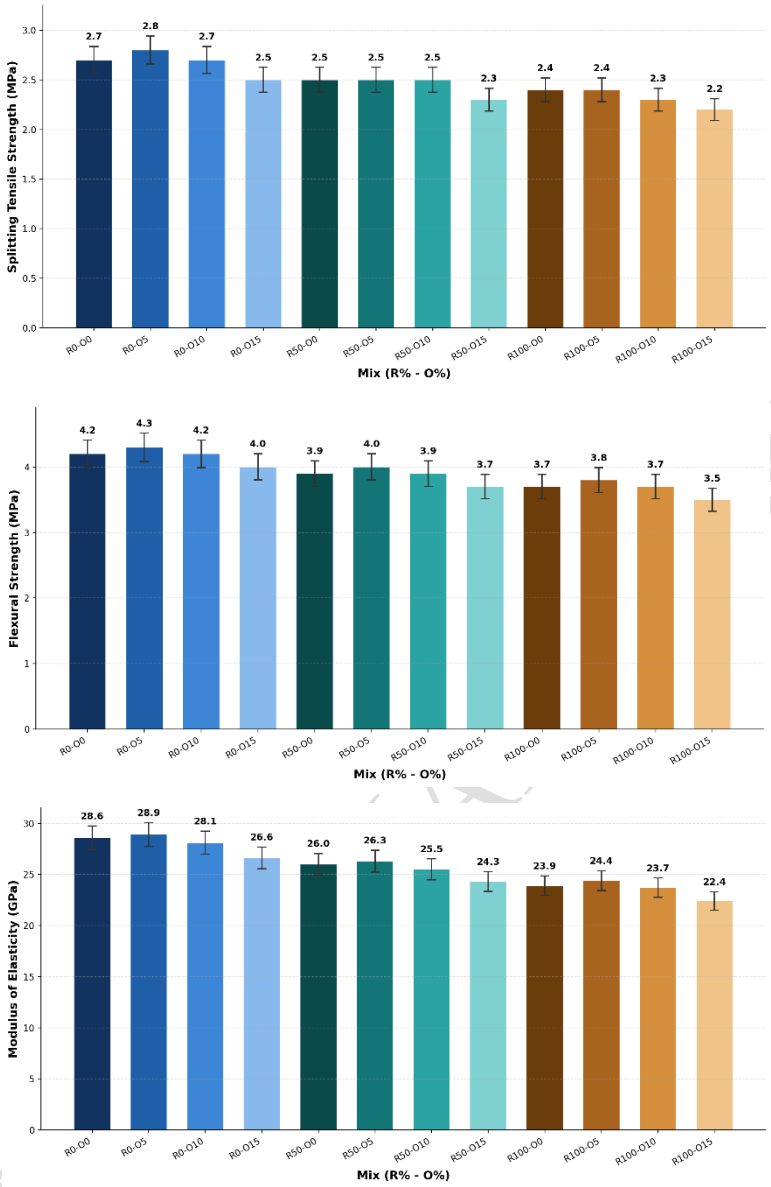


Figure 7 28-day splitting tensile strength, flexural strength, and modulus of elasticity (IC).

3.4. Durability Properties

Water permeability increased with RCA content, from 5.2 × 10^{-12} m/s (R0-O0 WC) to 11.2 × 10^{-12} m/s (R100-O15 WC), a 115% increase reflecting the porous microstructure of RCA and the cumulative effect of multiple ITZs in fully recycled mixes [21]. The substitution of 5% OOA reduced permeability by 7.7–10.5% relative to the 0% OOA control in each RCA group under WC, while 15% OOA increased it by 6.7–8.9%. Under IC, all permeability values were lower by 1.9–8.6% compared to their WC counterparts, with the greatest improvements at 100% RCA (R100-O0: 10.5 WC vs. 9.6 IC, −8.6%; R100-O5: 9.5 vs. 8.6, −9.5%).

Total porosity followed a pattern consistent with permeability, ranging from 9.8% (R0-O5 IC) to 17.2% (R100-O15 WC). IC reduced porosity by 2.0–8.1% relative to WC across the matrix. The mechanism involves the continued hydration products filling capillary pores during the extended curing period sustained by internal water release [4].

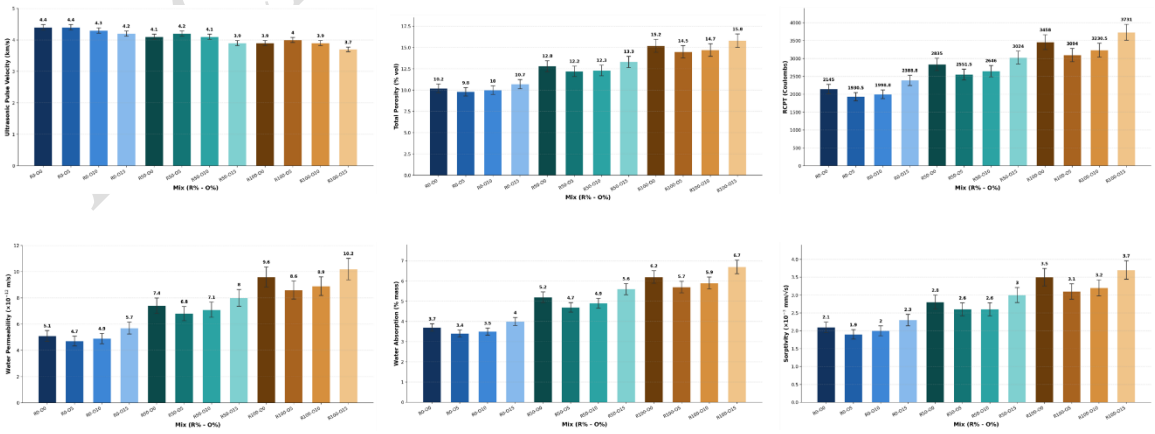
RCPT values under WC ranged from 1,980 Coulombs (R0-O5, classified as moderate chloride penetrability per ASTM C1202) to 4,100 Coulombs (R100-O15, high penetrability). IC reduced RCPT by 2.5–9.0% across all mixtures, with R100-O5 dropping from 3,400 (WC) to 3,094 (IC), a decrease of 306 Coulombs. The 5% OOA replacement consistently yielded the lowest RCPT within each RCA group under both curing regimes, attributable to the pozzolanic consumption of portlandite and consequent pore refinement [8, 10].

Water absorption and initial sorptivity exhibited similar dependence on RCA content and OOA dosage. Absorption increased from 3.5% (R0-O5 WC) to 7.3% (R100-O15 WC), while sorptivity ranged from 2.0 × 10^{-3} mm/√s (R0-O5 WC) to 4.0 × 10^{-3} mm/√s (R100-O15 WC). IC consistently reduced both metrics by 2.8–8.1%, reinforcing the conclusion that sustained internal hydration densifies the capillary pore network.

Table 5*. Selected durability properties under WC and IC

Mix (R% – O%)	Water Absorption (% mass)		Total Porosity (% vol)		RCPT (Coulombs)	
	WC	IC	WC	IC	WC	IC
R0-O0	3.8 ± 0.21	3.7 ± 0.21	10.5 ± 0.58	10.2 ± 0.57	2200 ± 150	2145 ± 140
R0-O5	3.5 ± 0.20	3.4 ± 0.20	10.0 ± 0.56	9.8 ± 0.54	1980 ± 130	1930.5 ± 130
R0-O10	3.6 ± 0.20	3.5 ± 0.20	10.3 ± 0.58	10.0 ± 0.56	2050 ± 140	1998.8 ± 135
R0-O15	4.1 ± 0.23	4.0 ± 0.22	11.0 ± 0.60	10.7 ± 0.59	2450 ± 165	2388.8 ± 155
R50-O0	5.5 ± 0.30	5.2 ± 0.29	13.5 ± 0.72	12.8 ± 0.69	3000 ± 190	2835 ± 185
R50-O5	5.0 ± 0.27	4.7 ± 0.26	12.8 ± 0.70	12.2 ± 0.67	2700 ± 180	2551.5 ± 165
R50-O10	5.2 ± 0.28	4.9 ± 0.27	13.0 ± 0.70	12.3 ± 0.67	2800 ± 185	2646 ± 170
R50-O15	5.9 ± 0.32	5.6 ± 0.30	14.0 ± 0.76	13.3 ± 0.70	3200 ± 205	3024 ± 195
R100-O0	6.8 ± 0.37	6.2 ± 0.34	16.5 ± 0.90	15.2 ± 0.82	3800 ± 245	3458 ± 220
R100-O5	6.2 ± 0.33	5.7 ± 0.31	15.8 ± 0.86	14.5 ± 0.78	3400 ± 215	3094 ± 200
R100-O10	6.4 ± 0.35	5.9 ± 0.32	16.0 ± 0.86	14.7 ± 0.80	3550 ± 225	3230.5 ± 205
R100-O15	7.3 ± 0.39	6.7 ± 0.36	17.2 ± 0.92	15.8 ± 0.85	4100 ± 260	3731 ± 240

*Values are expressed as mean ± SD (n = 3)



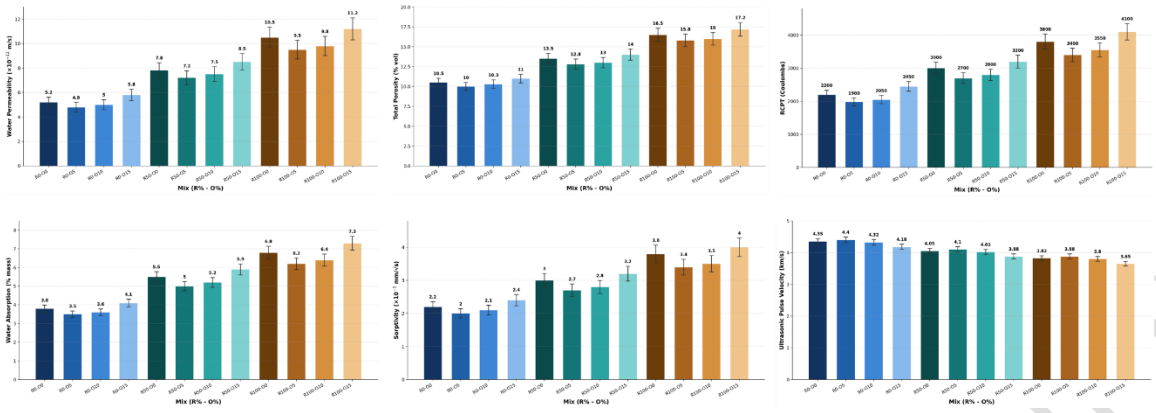


Figure 8: Durability properties: water permeability, total porosity, RCPT, water absorption, sorptivity, and UPV.

3.5. Ultrasonic Pulse Velocity and Hardened Density

UPV at 28 days decreased from 4.35 km/s (R0-O0 WC) to 3.65 km/s (R100-O15 WC), consistent with the increased porosity and weaker ITZs in RCA concrete. According to the quality classification by Whitehurst (1951), all R0 mixes fall in the "good" category (>4.0 km/s), while R100 mixes with 10–15% OOA under WC approach the "medium" threshold (<3.66 km/s). IC increased UPV by 0.02–0.08 km/s, with the pattern of improvement consistent with the densification inferred from porosity and permeability data. The 5% OOA replacement uniformly yielded the highest UPV within each RCA group, corroborating the beneficial pore-refinement effect observed across all durability indicators.

Hardened density followed fresh density trends, decreasing with both RCA and OOA content. IC specimens exhibited slightly higher densities (by 4.6–22.0 kg/m³) than their WC counterparts, consistent with additional hydration product formation.

3.6. Shrinkage Properties

Drying shrinkage at 28 days under WC increased from 365 $\mu\varepsilon$ (R0-O5) to 540 $\mu\varepsilon$ (R100-O15), representing a 48% increase. At 56 days, the range expanded to 470–685 $\mu\varepsilon$. The higher shrinkage of RCA mixes is attributed to the lower restraining capacity of porous recycled particles and the higher paste-to-aggregate stiffness ratio [22, 27]. The 5% OOA replacement reduced drying shrinkage by 3.1–4.7% relative to the 0% OOA control at both ages, while 15% OOA increased it by 4.2–6.3%.

IC significantly mitigated drying shrinkage: reductions ranged from 2.9% (R0-O0) to 8.0% (R100-O15) at 28 days and 2.7–8.0% at 56 days. The mechanism is directly linked to the release of absorbed water from RCA pores into the surrounding paste, which maintains a higher internal relative humidity and delays the onset of capillary stress-driven shrinkage [5, 6].

ACCEPTED MANUSCRIPT

Autogenous shrinkage at 7 days under WC ranged from 78 $\mu\varepsilon$ (R0-O5) to 115 $\mu\varepsilon$ (R100-O15). IC reduced autogenous shrinkage by 3.1–12.0%, with the greatest reduction in R100-O0 (108 $\mu\varepsilon$ WC vs. 95 $\mu\varepsilon$ IC, −12.0%). This reduction confirms that the internal water reservoir effectively counteracts the chemical shrinkage-driven self-desiccation that occurs during cement hydration in the early age period [5].

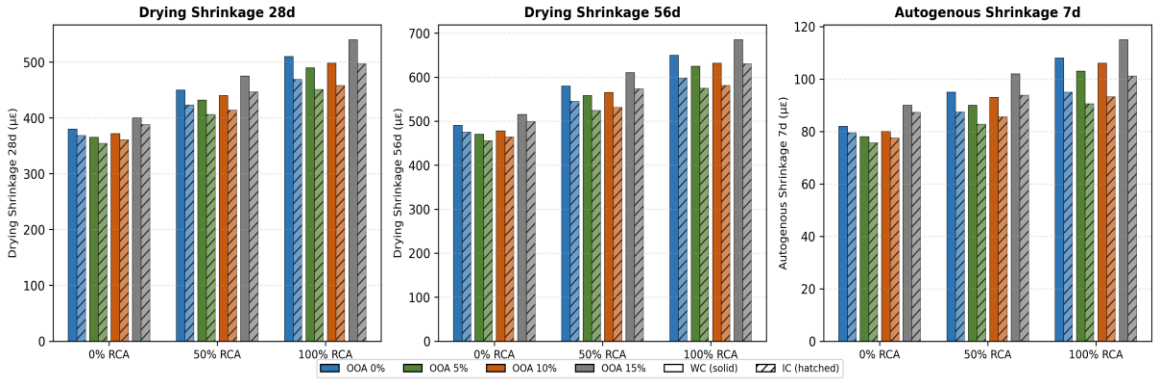


Figure 9: Drying shrinkage (28d and 56d) and autogenous shrinkage (7d) (solid = WC, hatched = IC).

3.7. Percentage Improvement of Internal Curing over Water Curing

To provide a concise quantitative comparison, Figure 10 presents the percentage change in key properties when IC is compared to WC for each of the 12 mixtures. Positive values indicate improvement (higher strength or lower RCPT/shrinkage). The compressive strength at 28 days showed consistent positive improvements of 0.9–7.5%, with the magnitude increasing at higher RCA levels. Splitting tensile strength improved by 0–9.1%, with the maximum gain observed at R100-O5. RCPT reductions ranged from 2.4 to 9.0%, while drying shrinkage at 28 days decreased by 2.9–8.0%. These results confirm that IC is particularly effective for high-RCA concretes containing moderate OOA levels.

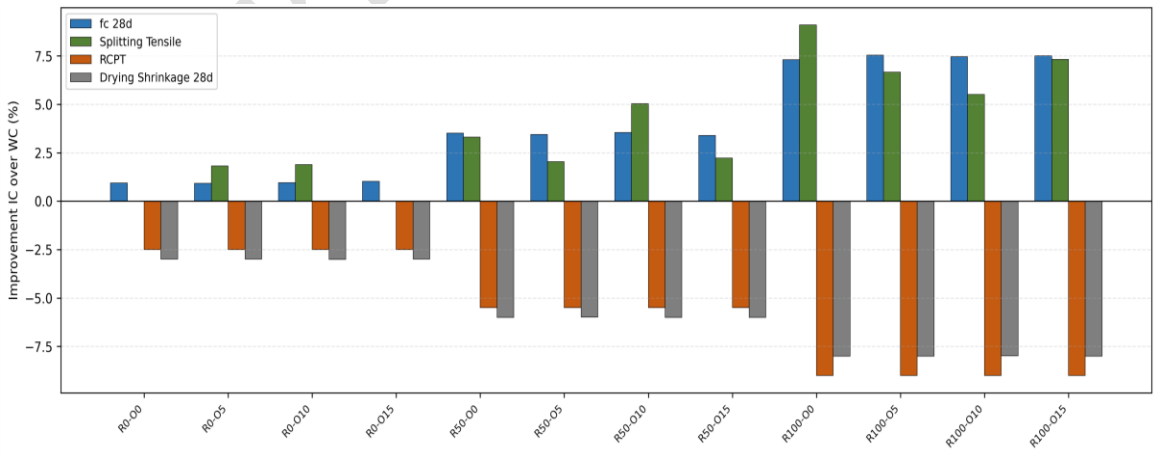


Figure 10: Percentage change in key properties: IC relative to WC (positive = improvement).

3.8. XRD Analysis

The X-ray diffraction patterns for all 24 mixtures at 28 days are presented in Figures 11–16. The principal crystalline phases identified across all specimens included portlandite (CH; primary peaks at 2θ = 18.0° and 34.1°), quartz/silica (SiO_2; peaks at 2θ = 20.9° and 26.6°), and alite/belite residuals contributing to the broad diffraction region at approximately 29–32°. The broad diffraction feature centred at approximately 29–32° was considered consistent with the presence of poorly crystalline hydration products, including C–S–H, although this region may overlap with residual clinker phases and calcite [29,30]. Although a full Rietveld refinement was not performed due to the predominantly amorphous nature of hydrated cement paste, a qualitative comparison of relative peak intensities was conducted by normalizing the CH (18.0°) and the broad feature near 29.4° to the quartz peak at 26.6°. This normalization was used only to facilitate comparison among diffraction patterns and was not considered a quantitative measure of phase abundance.

Across the WC specimens (Figure 11), the apparent CH peak intensity at 18.0° showed a progressive decrease with increasing OOA content from 0% to 5%, a trend qualitatively consistent with possible CH consumption, although it cannot independently confirm a pozzolanic reaction. However, at 10% and 15% OOA, the CH peak intensity was only marginally lower than at 0% OOA, while the SiO_2-related peaks at 20.9° and 26.6° intensified appreciably. These changes may reflect differences in the crystalline silica contribution from OOA; however, they should be interpreted cautiously and cannot independently establish the extent of pozzolanic reaction. The broad diffraction feature in the 29–32° region was more pronounced for the 5% OOA mixes, qualitatively supporting, but not independently confirming, the trends observed in the mechanical and durability results.

The effect of RCA replacement level on the diffraction patterns was subtle. Mixes with 50% and 100% RCA exhibited slightly broader and less intense features in the 29–32° region compared to their 0% RCA counterparts at the same OOA level, which may be associated with differences in the composition and heterogeneity introduced by the adhered mortar in RCA concrete. The CH peaks were marginally higher in RCA mixes, which may be associated with residual portlandite originating from the old adhered mortar [24].

Comparison of WC and IC specimens (Figures 12–15) revealed differences in the apparent intensities of the CH, silica-related, and broad hydration-product features. The generally lower apparent CH intensity and more pronounced broad feature in the 29–32° region observed in some IC mixtures are qualitatively consistent with continued hydration and possible additional reaction in the presence of internal moisture. However, these observations do not independently establish the extent of CH consumption or C–S–H formation. Overall, the XRD observations provide qualitative, corroborative evidence consistent with the macroscopic trends reported in Sections 3.2–3.6.

ACCEPTED MANUSCRIPT

Several limitations of the XRD analysis should be acknowledged when interpreting these observations. First, C–S–H is a poorly crystalline to amorphous phase that produces a broad, diffuse hump (approximately 29–32°) overlapping with residual C_3S/C_2S reflections and calcite; consequently, the small differences in apparent peak intensity at 29.4° cannot be regarded as a quantitative measure of C–S–H content. Second, the quartz reflection at 26.6° used here for normalisation is not necessarily constant across mixtures, because the quartz content of the RCA-attached mortar differs from that of the NCA limestone; the use of quartz as an internal standard may therefore introduce a systematic bias. Third, XRD was the only microstructural technique employed, and neither Rietveld refinement nor quantitative phase analysis was performed. For these reasons, the XRD results are interpreted here as qualitative, corroborative evidence only, and the mechanistic inferences regarding additional pozzolanic reaction and C–S–H formation should be regarded as tentative. Complementary techniques, including thermogravimetric analysis (TGA) for quantitative CH consumption, SEM-EDS for ITZ morphology and elemental mapping, and mercury intrusion porosimetry (MIP) or BET analysis for pore-size distribution, would be required to establish these mechanisms more conclusively and are recommended for future work.

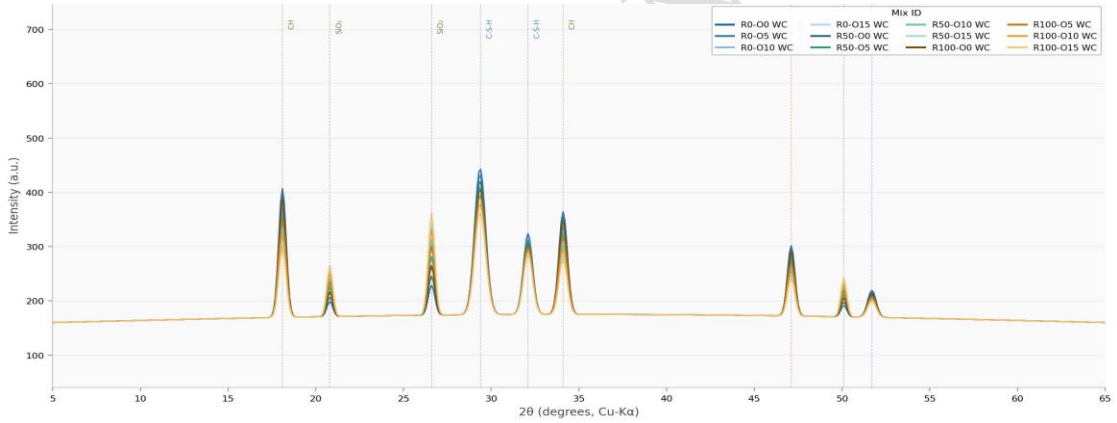


Figure 11: XRD patterns of all 12 water-cured specimens at 28 days.

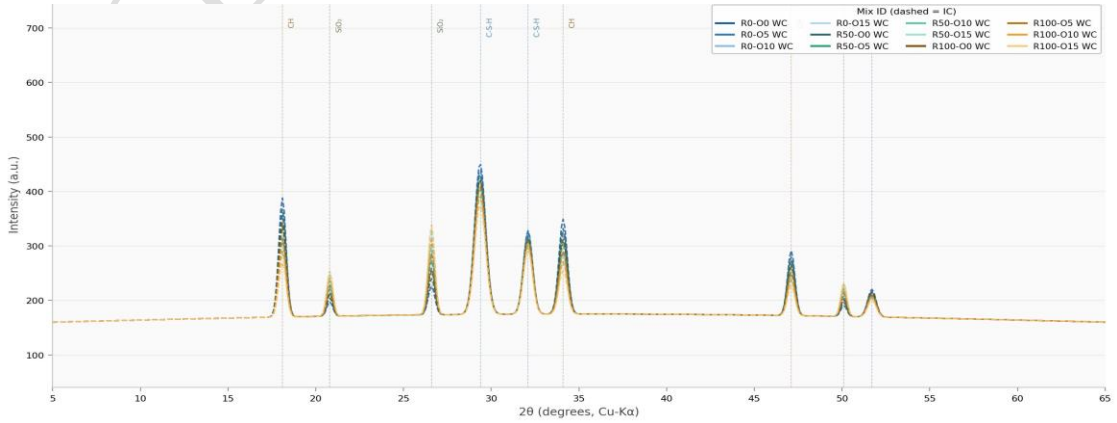


Figure 12: XRD patterns of all 12 internally-cured specimens (dashed) overlaid with WC (solid).

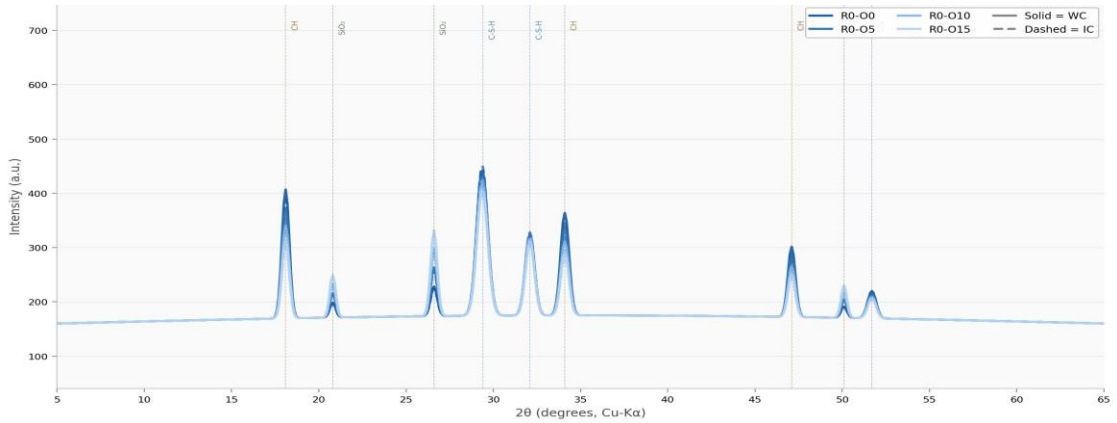


Figure 13: XRD comparison of WC vs IC for R0 group (0% RCA).

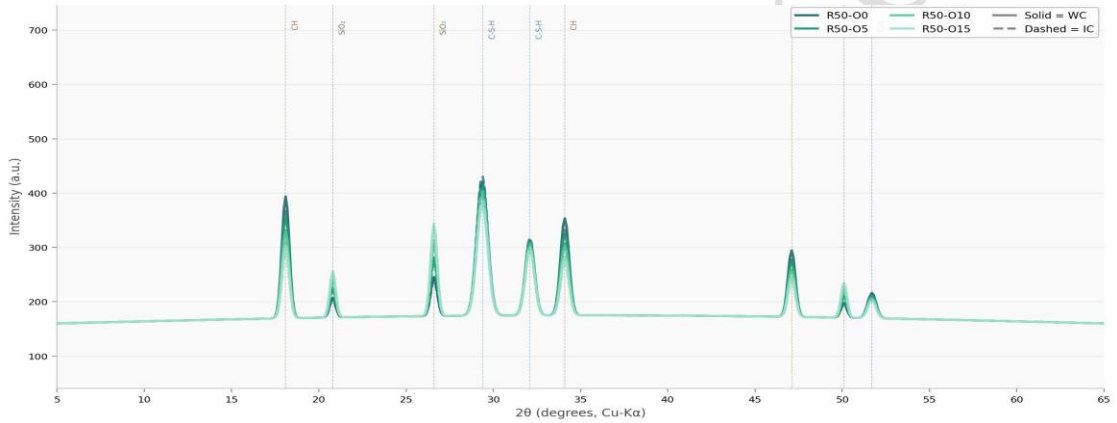


Figure 14: XRD comparison of WC vs IC for R50 group (50% RCA).

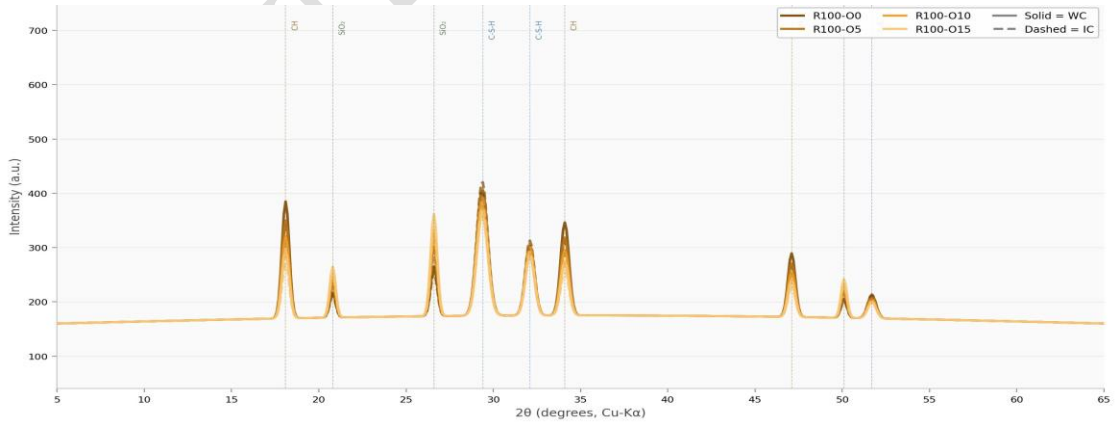


Figure 15: XRD comparison of WC vs IC for R100 group (100% RCA).

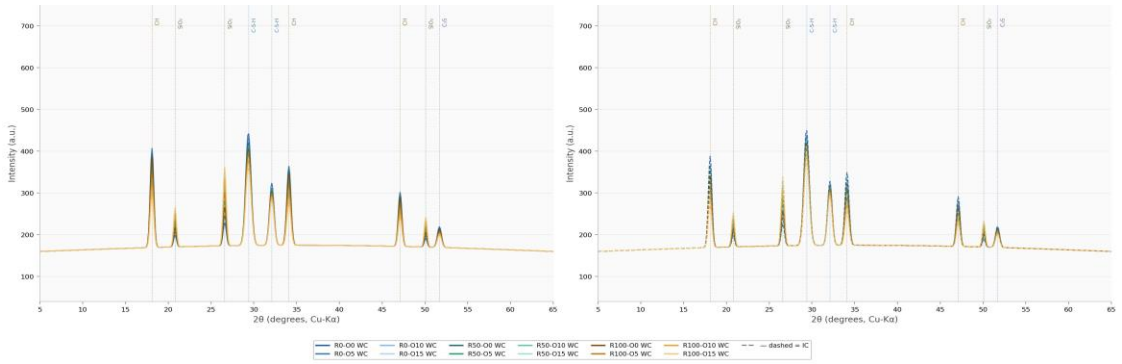


Figure 16: Combined WC (left) and WC vs IC (right) XRD patterns for all 24 mixtures.

4. Integrated Discussion and Practical Implications

The experimental evidence establishes three principal findings with direct implications for sustainable concrete design. First, 5% OOA replacement represents an optimal dosage that enhances or maintains all measured properties across the full range of RCA levels (0–100%) and under both curing regimes. The observed performance at this dosage may be associated with filler effects and possible additional reaction of OOA. The XRD patterns provide only qualitative, corroborative evidence consistent with possible CH consumption and the presence of poorly crystalline hydration products; they do not independently confirm additional C–S–H formation (see the limitations discussed in Section 3.8). At 10% OOA, the measured performance suggests that the potential benefits of OOA become increasingly offset by clinker dilution, resulting in negligible net effects. At 15% OOA, the measured results indicate that the dilution effect becomes more influential, producing measurable reductions in strength (5–8%) and durability (7–15% increase in permeability-related indices). The corresponding XRD changes should be regarded as qualitative observations rather than direct evidence of unreacted silica accumulation.

The fractured surface of a representative RCA concrete specimen (R100-O5) is presented in Figure 17, where the adhered mortar layer surrounding original aggregate particles and the multiple interfacial transition zones are clearly visible. The darker cement paste matrix and lighter aggregate particles with residual mortar demonstrate the heterogeneous microstructure characteristic of RCA concrete, which underpins the mechanical and durability performance differences reported in this study.

ACCEPTED MANUSCRIPT



Figure 17: Cross-section of RCA concrete specimen (R100-O5) showing aggregate particles with adhered mortar and multiple interfacial transition zones.

Second, internal curing is more beneficial in the tested RCA-rich mixtures than in the corresponding natural-aggregate mixtures. The improvements in 56-day compressive strength ranged from 0.9% (R0-O0) to 9.2% (R100-O5), with similar trends observed for several durability metrics. This is consistent with the greater amount of pre-absorbed water available at higher RCA contents, providing a larger potential internal moisture reservoir. The dual role of RCA as both aggregate and a potential internal moisture reservoir may therefore provide a practical advantage when pre-saturation is appropriately controlled.

A methodological consideration specific to the internally cured mixtures concerns the fate of the water pre-absorbed by the RCA. For the R100 group, the approximately 44.7 kg/m³ of internal water is not distributed uniformly throughout the paste; rather, it is released locally from the RCA pores into the surrounding cement paste, which may temporarily modify the local moisture conditions and effective water-to-binder ratio near the RCA–paste interface, while the bulk paste farther from the aggregate retains a ratio close to the nominal effective w/b value of 0.45. Two competing consequences may therefore occur. On one hand, the released internal water may help maintain local moisture availability and support continued hydration. On the other hand, local water release may alter the effective water-to-binder ratio near the ITZ and could potentially influence its initial porosity. The net experimental outcome for the IC specimens—lower permeability, porosity, and RCPT together with higher later-age strength—is consistent with a beneficial contribution from sustained internal hydration; however, these bulk measurements alone cannot establish whether this mechanism dominates over possible adverse effects associated with locally elevated water availability. Nevertheless, because these two effects cannot be fully deconvoluted from bulk measurements

ACCEPTED MANUSCRIPT

alone, the present data do not permit a definitive separation of the contribution of sustained internal hydration from that of local changes in water availability near the RCA–paste interface; targeted characterisation of the ITZ (for example, SEM-EDS or micro-computed tomography) would be required to resolve this question and is recommended for future work.

Third, the combined effect of OOA and IC was most favourable at the 5% OOA level based on the measured macroscopic properties. The additional moisture provided by IC may support continued hydration and potentially extend the reaction period of OOA. The XRD observations, including differences in the apparent CH intensity and the broad feature in the 29–32° region between IC and WC specimens, are qualitatively consistent with this interpretation but do not independently confirm greater portlandite consumption or C–S–H formation. At 15% OOA, the measured performance indicates that IC was insufficient to fully offset the reduction associated with the higher OOA replacement level.

From a practical standpoint, these findings demonstrate the potential of concrete incorporating 100% RCA and 5% OOA under internal curing. The R100-O5-IC mix achieved a 56-day compressive strength of 32.2 MPa, total porosity of 14.5%, and RCPT of 3,094 Coulombs. While this strength level classifies the concrete as normal-strength rather than high-performance, it is important to note that the water-to-binder ratio of 0.45 and total binder content of 380 kg/m³ were deliberately selected to represent typical structural concrete proportions rather than optimized high-strength formulations. The present results therefore demonstrate the mechanical and durability performance achieved under the investigated mixture proportions, while broader structural applicability should be evaluated according to the relevant design and durability requirements. Future investigations could examine lower w/b ratios and higher binder contents to determine whether higher strengths can be achieved while maintaining the beneficial trends observed in this study. The R100-O5-IC mixture showed values approaching those of R50-O0-WC (31.0 MPa, 13.5%, 3,000 Coulombs). This suggests that the combined use of 5% OOA and IC may partially compensate for the performance reduction associated with increasing RCA content, with potential implications for waste utilization and circular-economy approaches in concrete production.

A preliminary carbon-emission assessment indicated a potential CO_2 reduction of approximately 18% for the optimized R100-O5-IC mixture compared with the conventional reference under the adopted assumptions. This value should be interpreted as a scenario-dependent, cradle-to-gate estimate rather than a definitive life-cycle reduction because it is sensitive to the adopted emission factors and avoided-disposal assumptions and does not fully account for OOA grinding, PCE production, transportation, and other processing burdens. A comprehensive LCA with region-specific inventory data and sensitivity analysis is therefore required before firm environmental-benefit claims are made.

ACCEPTED MANUSCRIPT

Sustainability Assessment and CO_2 Reduction Potential

A preliminary carbon-emission estimate was conducted to explore the potential environmental benefits of the optimized mixture. Using published emission factors (OPC: 0.93 kg CO_2/kg; NCA extraction and processing: 0.0048 kg CO_2/kg; RCA processing: 0.0024 kg CO_2/kg; OOA was initially assigned a zero upstream production burden as a waste by-product, while its subsequent processing impacts were not included in the preliminary calculation), the embodied CO_2 of each mixture was estimated per cubic metre of concrete. The reference mixture R0-O0 produces approximately 353 kg CO_2/m³ from binder alone (380 kg OPC × 0.93). The optimized R100-O5-IC mixture, with 361 kg OPC and 19 kg OOA, reduces the binder-related CO_2 to approximately 336 kg CO_2/m³, a 5% reduction from cement replacement alone. Additionally, the complete substitution of NCA with RCA reduces the calculated aggregate-related contribution from approximately 4.6 kg CO_2/m³ for NCA to approximately 2.3 kg CO_2/m³ for RCA processing, based on the adopted emission factors. When an assumed avoided-disposal credit of 0.05 kg CO_2/kg is applied to CDW and OOA, the estimated total CO_2 reduction is approximately 18% compared to the conventional R0-O0-WC reference. However, this value represents a scenario-dependent preliminary estimate rather than a definitive life-cycle reduction and is highly dependent on the adopted emission factors and avoided-disposal assumptions [38].

The scope and limitations of this assessment must be stated explicitly. The analysis adopts a simplified cradle-to-gate boundary and does not constitute a full life-cycle assessment. Several factors are not captured and could affect the estimated net environmental benefit: (i) the energy consumed in grinding OOA to a median particle size of 50 μm (specific surface area ≈ 25 m²/g), which was not included in the preliminary calculation and therefore prevents OOA from being treated as strictly carbon-neutral after processing; (ii) the embodied carbon associated with the near-threefold increase in PCE superplasticizer dosage (from 0.40% to 1.15% by binder mass) in the high-replacement mixtures; and (iii) transportation, RCA crushing and processing, and the additional handling associated with RCA pre-saturation for internal curing. Furthermore, the emission factors adopted, including RCA processing at 0.0024 kg CO_2/kg, NCA at 0.0048 kg CO_2/kg, and the avoided-landfill credit of 0.05 kg CO_2/kg applied to both CDW and olive-pomace ash, are representative literature values whose regional applicability to the Malaysian context has not been verified. The use of a common avoided-disposal factor for two different waste streams also introduces additional uncertainty. The reported reduction is particularly sensitive to the avoided-landfill assumption: replacing cement with 5% OOA alone accounts for only about a 5% reduction in binder-related CO_2, so a substantial part of the headline figure derives from the avoided-disposal credit. Accordingly, the reported 18% reduction should be interpreted only as a preliminary scenario estimate. A more comprehensive LCA using region-specific inventory data and incorporating transportation, OOA grinding, PCE production,

ACCEPTED MANUSCRIPT

RCA processing, and sensitivity analysis is required before definitive environmental-benefit claims can be made.

The preliminary environmental benefit was achieved while maintaining the measured mechanical performance: the R100-O5-IC mix attained a 56-day compressive strength of 32.2 MPa. Together with the use of RCA and OOA as recycled and waste-derived constituents, these results indicate the potential of the optimized mixture to reduce reliance on virgin materials and OPC while maintaining useful mechanical performance. However, its overall environmental advantage should be confirmed through a comprehensive life-cycle assessment incorporating the additional processing, transportation, admixture, and regional factors discussed above.

5. Conclusions

Based on the comprehensive experimental investigation of 24 concrete mixtures encompassing three RCA levels, four OOA dosages, and two curing regimes, the following conclusions are drawn:

(1) Increasing RCA replacement from 0% to 100% reduced 28-day compressive strength by 18.8%, splitting tensile strength by 18.5%, flexural strength by 16.7%, and modulus of elasticity by 19.3% under water curing, while increasing water permeability by 102%, porosity by 57%, RCPT by 73%, and drying shrinkage by 34%.

(2) OOA at 5% replacement improved 28-day compressive strength by 1.6–1.9%, splitting tensile strength by 1.4–2.3%, and all durability indicators by 3–11% relative to the 0% OOA control across all RCA levels. At 15% OOA, all properties deteriorated by 5–15%.

(3) Internal curing enhanced 56-day compressive strength by 0.9–9.2%, with the greatest gains in 100% RCA concretes. IC also reduced water permeability by 1.9–8.6%, porosity by 2.0–8.1%, RCPT by 2.5–9.0%, drying shrinkage by 2.7–8.0%, and autogenous shrinkage by 3.1–12.0%.

(4) XRD analysis provided qualitative evidence consistent with pozzolanic consumption of portlandite and enhanced C–S–H formation at 5% OOA, while higher OOA levels lead to unreacted silica accumulation. IC specimens exhibited more complete hydration with lower CH and higher C–S–H peak intensities compared to WC specimens.

(5) The combination of 100% RCA, 5% OOA, and internal curing produced 56-day properties (fc = 32.2 MPa, porosity = 14.5%, RCPT = 3,094 C) comparable to 50% RCA concrete without OOA under water curing, demonstrating that this synergistic approach can offset the full RCA replacement penalty.

These results provide a strong basis for specifying OOA-blended, internally cured RCA concrete in structural applications where sustainability, waste utilization, and adequate durability are required. Future

ACCEPTED MANUSCRIPT

research should investigate the long-term durability (carbonation, sulfate resistance, freeze-thaw) and the life-cycle environmental assessment of the optimized mixtures. Additional studies employing scanning electron microscopy with energy-dispersive X-ray spectroscopy (SEM-EDS) and thermogravimetric analysis (TGA) are recommended to provide quantitative microstructural characterization of the ITZ and hydration product assemblages. Rietveld refinement of XRD data, combined with selective dissolution techniques, would enable more precise quantification of the pozzolanic reaction extent at each OOA dosage. Statistical design of experiments (e.g., response surface methodology) could further optimize the mixture proportions while reducing the number of required trial batches.

Compliance with Ethical Standards

Conflict of Interest

The author declares that there are no conflicts of interest regarding the publication of this paper.

Research Involving Human Participants and/or Animals

This study does not involve any human participants or animals.

Informed Consent

Not applicable.

Author's Contributions

Author #1 Siwar Khasawneh：Drafted and wrote the manuscript, performed the experiment and result analysis

Author #2 Ayat Khasawneh: Assisted in analytical analysis on the structure

Data Availability

The data that support the findings of this study are available from the corresponding author upon reasonable request.

Funding Statement

This research did not receive any specific grant from funding agencies in the public, commercial, or not-for-profit sectors.

Dataset

All data generated or analyzed during this study are included in this published article. Additional data are available from the corresponding author upon reasonable request.

Copyright

ACCEPTED MANUSCRIPT

The authors confirm that the manuscript is original, has not been published previously, and is not under consideration for publication elsewhere. Upon acceptance, the authors agree to transfer the copyright of the article to the Journal of Sustainable Construction Materials and Technologies.

References

[1] V. Tam, C.M. Tam, K.N. Le, "Removal of cement mortar remains from recycled aggregate using pre-soaking approaches," Resources, Conservation and Recycling, vol. 50, no. 1, pp. 82–97, 2007.

[2] M. Etxeberria, E. Vázquez, A. Marí, M. Barra, "Influence of amount of recycled coarse aggregates and production process on properties of recycled aggregate concrete," Cement and Concrete Research, vol. 37, no. 5, pp. 735–742, 2007.

[3] C.S. Poon, Z.H. Shui, L. Lam, H. Fok, S.C. Kou, "Influence of moisture states of natural and recycled aggregates on the slump and compressive strength of concrete," Cement and Concrete Research, vol. 34, no. 1, pp. 31–36, 2004.

[4] D. Bentz, W. Weiss, "Internal curing: A 2010 state-of-the-art review," NISTIR 7765, National Institute of Standards and Technology, 2011.

[5] P. Lura, O.M. Jensen, K. van Breugel, "Autogenous shrinkage in high-performance cement paste: An evaluation of basic mechanisms," Cement and Concrete Research, vol. 33, no. 2, pp. 223–232, 2003.

[6] J. Castro, L. Keiser, M. Golias, W. Weiss, "Absorption and desorption properties of fine lightweight aggregate for application to internally cured concrete mixtures," Cement and Composites, vol. 33, no. 10, pp. 1001–1008, 2011.

[7] R. Siddique, J. Klaus, "Influence of metakaolin on the properties of mortar and concrete: A review," Applied Clay Science, vol. 43, no. 3–4, pp. 392–400, 2009.

[8] M. Thomas, "Supplementary cementing materials in concrete," CRC Press, 2013.

[9] K.H. Yang, Y.B. Jung, M.S. Cho, S.H. Tae, "Effect of supplementary cementitious materials on reduction of CO_2 emissions from concrete," Journal of Cleaner Production, vol. 103, pp. 774–783, 2015.

[10] F.P. Cota, C.D.R. Melo, T.H. Panzera, A.G. Araújo, P.H.R. Borges, F. Rubio, "Mechanical properties and ASR evaluation of concrete with ashes from agricultural waste," Construction and Building Materials, vol. 74, pp. 184–190, 2015.

[11] ASTM C33, "Standard specification for concrete aggregates," ASTM International, West Conshohocken, PA, 2023.

ACCEPTED MANUSCRIPT

[12] ASTM C150, "Standard specification for portland cement," ASTM International, West Conshohocken, PA, 2022.

[13] ASTM C39, "Standard test method for compressive strength of cylindrical concrete specimens," ASTM International, 2021.

[14] ASTM C496, "Standard test method for splitting tensile strength of cylindrical concrete specimens," ASTM International, 2017.

[15] ASTM C78, "Standard test method for flexural strength of concrete," ASTM International, 2022.

[16] ASTM C469, "Standard test method for static modulus of elasticity and Poisson's ratio of concrete in compression," ASTM International, 2022.

[17] ASTM C1202, "Standard test method for electrical indication of concrete's ability to resist chloride ion penetration," ASTM International, 2022.

[18] ASTM C1585, "Standard test method for measurement of rate of absorption of water by hydraulic-cement concretes," ASTM International, 2020.

[19] ASTM C157, "Standard test method for length change of hardened hydraulic-cement mortar and concrete," ASTM International, 2017.

[20] ASTM C597, "Standard test method for pulse velocity through concrete," ASTM International, 2022.

[21] S. Kou, C. Poon, "Enhancing the durability properties of concrete prepared with coarse recycled aggregate," Construction and Building Materials, vol. 35, pp. 69–76, 2012.

[22] J. Xiao, J. Li, C. Zhang, "Mechanical properties of recycled aggregate concrete under uniaxial loading," Cement and Concrete Research, vol. 35, no. 6, pp. 1187–1194, 2005.

[23] A. Katz, "Properties of concrete made with recycled aggregate from partially hydrated old concrete," Cement and Concrete Research, vol. 33, no. 5, pp. 703–711, 2003.

[24] W. Li, J. Xiao, Z. Sun, S. Kawashima, S.P. Shah, "Interfacial transition zones in recycled aggregate concrete," Cement and Concrete Composites, vol. 34, no. 2, pp. 224–232, 2012.

[25] D. Pedro, J. de Brito, L. Evangelista, "Influence of the use of recycled concrete aggregates from different sources on structural concrete," Construction and Building Materials, vol. 71, pp. 141–151, 2014.

[26] R.V. Silva, J. de Brito, R.K. Dhir, "Properties and composition of recycled aggregates from construction and demolition waste suitable for concrete production," Construction and Building Materials, vol. 65, pp. 201–217, 2014.

ACCEPTED MANUSCRIPT

[27] M.C.S. Nepomuceno, R.A.S. Isidoro, J.P.G. Catarino, "Mechanical performance evaluation of concrete made with recycled ceramic coarse aggregates from industrial brick waste," Construction and Building Materials, vol. 165, pp. 284–294, 2018.

[28] P. Mehta, P. Monteiro, "Concrete: Microstructure, Properties, and Materials," 4th ed., McGraw-Hill, 2014.

[29] H.F.W. Taylor, "Cement Chemistry," 2nd ed., Thomas Telford, London, 1997.

[30] I. Odler, "Special Inorganic Cements," E & FN Spon, London, 2000.

[31] S. Pradhan, S. Kumar, S.V. Barai, "Recycled aggregate concrete: Particle packing method (PPM) of mix design approach," Construction and Building Materials, vol. 152, pp. 269–284, 2017.

[32] J. Zhang, C. Shi, Y. Li, X. Pan, C. Poon, Z. Xie, "Influence of carbonated recycled concrete aggregate on properties of cement mortar," Construction and Building Materials, vol. 98, pp. 1–7, 2015.

[33] R. Hay, K. Celik, "Accelerated carbonation of reactive magnesium oxide cement (RMC)-based composite with supercritical carbon dioxide ($scCO_2$)," Journal of Cleaner Production, vol. 248, p. 119282, 2020.

[34] M.S. de Juan, P.A. Gutiérrez, "Study on the influence of attached mortar content on the properties of recycled concrete aggregate," Construction and Building Materials, vol. 23, no. 2, pp. 872–877, 2009.

[35] European Committee for Standardization, EN 206:2013+A2:2021, "Concrete — Specification, performance, production and conformity," CEN, Brussels, 2021.

[36] P.K. Mehta, R.W. Burrows, "Building durable structures in the 21st century," Indian Concrete Journal, vol. 75, no. 7, pp. 437–443, 2001.

[37] IEA and WBCSD, "Technology Roadmap — Low-Carbon Transition in the Cement Industry," International Energy Agency, Paris, 2018.

[38] A. Yazdanbakhsh, M. Lagouin, "The effect of geographic boundaries on the results of a regional life cycle assessment of using recycled aggregate in concrete," *Resources, Conservation and Recycling*, vol. 143, pp. 201–209, 2019.

ACCEPTED MANUSCRIPT